Diffusion of phosphorus in α-Fe: An *ab initio* study

C. Domain
Electricité de France, EDF Recherche et Développement, Dpt Matériaux et Mécanique des Composants, Les Renardières, F-77250 Moret sur Loing, France

C. S. Becquart
Laboratoire de Métallurgie Physique et Génie des Matériaux, Ecole Nationale Supérieure de Chimie de Lille, UMR 8517 Centre Nationale de la Recherche Scientifique—Université des Sciences et Technologies de Lille—Electricité de France, Bât. C6, F-59655 Villeneuve d'Ascq Cedex, France

(Received 10 January 2005; published 28 June 2005)

The occupation site and the behavior of the phosphorus atom in α iron is investigated by *ab initio* density functional theory based calculations. The interaction of P with vacancy and self-interstitial atoms is discussed. The migration energies associated to diffusion by vacancy mechanism are determined and the P diffusion coefficient in Fe is derived. The influence of P on point defect migration is analyzed, and in particular the trapping of self-interstitial atom and vacancy is discussed.

DOI: 10.1103/PhysRevB.71.214109 PACS number(s): 61.72.Ji, 71.15.Mb, 71.20.Be

I. INTRODUCTION

It is well known that the main effect of phosphorus is to promote embrittlement at grain boundaries (see for instance the thorough review by English *et al.*[1]). This intergranular embrittlement is due to phosphorus segregation (enhanced by thermal ageing or under neutron irradiation) at the grain boundaries.[2] P segregation has also been observed at dislocations or precipitate-matrix interface.[3] In addition, phosphorus was found to influence the evolution of the microstructure of Fe alloys under irradiation.[4] Atom probe analysis of neutron irradiated ferritic alloys have shown the presence of small phosphorus rich clusters, very diffuse, with 1–2 nm typical radius size associated or not with Cu or other solute atoms.[3,5]

The mechanisms responsible for the formation of these solute rich clusters are not yet elucidated. However, the interactions of the point defects induced by irradiation (vacancies and/or self-interstitial atoms) with the solute atoms must very probably be partly responsible of these phenomena.

Lidiard[6] has used the analytical expressions derived by Barbu and Lidiard[7] for the coupling between point defect fluxes to investigate phosphorus diffusion in Fe. This model requires the knowledge of physical properties not accurately known at the moment. In particular the interaction between a vacancy and a phosphorus atom was totally neglected, and only the coupling between self-interstitial atoms and phosphorus was considered.

Faulkner and coworkers[8] have modeled the phosphorus grain boundary segregation under neutron irradiation as a function of temperature. They used molecular dynamics results to obtain the amount of residual point defects by cascade for a given energy and thus determine the amount of freely migrating point defects produced by the irradiation. Their model predicts phosphorus segregation as a function of temperature and neutron spectrum. The number of freely migrating defects depends on the cascade energy and consequently directly on the spectrum, and the low energy part of the neutron spectrum was shown to have an important contribution to the segregation. In that case also, these authors assumed that only single self-interstitial atoms couple with P atoms for the transport of phosphorus solute atoms to grain boundaries.

The assumptions made by Faulkner and coworkers as well as by Lidiard very probably originate from the experimental finding that the P coefficient diffusion in body-centered cubic (bcc) Fe is high.[9]

Recently, Hardouin du Parc[10] measured the interstitial loop distributions and sizes in Fe as well as in FeP dilute alloy under high energy electron irradiation in a high voltage electron microscope. From their results, they evaluated effective vacancy and self-interstitial diffusion coefficients and found that the presence of phosphorus leads to an increase of the effective self-interstitial migration energy, thus corroborating the assumptions made previously. They also observe a decrease of the effective vacancy prefactor in $FeP_{0.11\%}$ and an increase of the effective migration energy of the vacancy in presence of phosphorus.

More recently Nagai and coworkers observed by positron annihilation studies that phosphorous promoted the formation of vacancy clusters during high energy electron irradiation of Fe.[11]

A good knowledge of P diffusion and its interaction with point defects in the α iron matrix is thus technologically crucial and is likely to improve the models dedicated to the study of the evolution of the microstructure under thermal ageing or irradiation.

Such studies have to be done at the atomistic level. Hashimoto *et al.*[12] used an Fe-P Morse potential to study the segregation of P in grain boundaries, while Vasiliev and coworkers[13] used the same potential to investigate at the atomistic level some phosphorus defects properties. The Morse potential has been used once more, along with the Ackland *et al.*[14] Fe potential to study point defect[15] and P interactions at grain boundaries.[16]

However, simulations based on empirical potentials have to be used with care as regards to interactions with point defects because these potentials are most of the time adjusted

on equilibrium properties. For instance, many of the Embedded Atom Method (EAM) type potentials dedicated to the study of α Fe do not predict correctly the stable configuration of the interstitials or the relative formation energies of the dumbbells. To our knowledge, the only empirical potentials which predict correctly interstitial properties are that derived by Mendelev and coworkers[17] and Ackland *et al.*,[18] but this is because the potential was adjusted on *ab initio* results,[19] some of them related to interstitial properties. Furthermore, empirical potentials most of the time lack information about the local or far from equilibrium chemistry of defect interactions.

For these reasons, Ackland and coworkers have very recently developed a FeP potential of the embedded atom method type, using some *ab initio* data as fitting parameters.[18] The interaction of phosphorus with one vacancy and in interstitial positions was determined, in the framework of the density functional theory, on very small supercells (16- and 32-atom supercells), and the data obtained used to fit the empirical potential.

Indeed, *ab initio* calculations based on the density functional theory (DFT) appear today to be the most appropriate tool to evaluate fine interactions between defects and solute atoms and can thus give a better understanding of the basic atomic phenomena involved in, for instance, the changes in the microstructure concurrent with irradiation. Calculations of this kind have shown, for example, that C and N interact strongly with vacancies in agreement with experimental data.[20] Along with their important role in the building of empirical potential, another use of the data thus obtained is their introduction in higher scale modeling such as rate theory models or kinetic Monte Carlo simulations.

To our knowledge, besides the calculations of Ackland *et al.* aimed at building an empirical potential,[18] previous *ab initio* calculations in the iron phosphorus system were devoted to surface and grain boundary interactions[21–25] and have focused on the strengthening of the bonds induced by the P atom at the interface.

Being considered as an undersized substitutional impurity,[26] P would in principle interact with both vacancies and interstitials. For this reason, in the work presented here, the interaction of P atoms with vacancies as well as with self-interstitial atoms is investigated.

In a preliminary part, the most stable occupation site of P is determined and compared to other possible sites. The interaction between P and point defects: Vacancy and self-interstitial atoms is determined. The migration energies involving P and a vacancy are given and discussed, the phosphorus diffusion coefficient based on a vacancy mechanism is evaluated.

II. METHODOLOGY

The *ab initio* calculations presented in this work are based on the density functional theory. They have been performed using the Vienna *ab initio* simulation package (VASP), see Refs. 27–29 and references therein. The calculations were done in a plane-wave basis, using fully nonlocal Vanderbilt type ultrasoft pseudopotentials (USPP)[30] to describe the electron-ion interaction, and within the spin polarized generalized gradient approximation (GGA) of Perdew and Wang.[31] The pseudopotentials were taken from the VASP library. For Fe, the six $3d$ electrons are considered as valence ones together with the two $4s$ (the reference state is more precisely $3d^{6.2}4s^{1.8}$). For P, five valence electrons are used: $3s$ and $3p$ (reference $3s^2 3p^3$). In addition, some calculations were done using the projector augmented wave (PAW) approach[32] as well as taking into account the Vosko and coworkers corrections for the exchange correlation.[33]

Periodic boundary conditions and the supercell approach were used for all calculations. Brillouin zone sampling was performed using the Monkhorst and Pack scheme.[34] The defect calculations were performed at constant volume thus relaxing only the atomic position in a supercell dimensioned with the equilibrium lattice parameter for the pure matrix (2.8544 Å for Fe in our case). This allows one to use a smaller plane-wave cutoff energy (240 eV). The calculations were done with 54-atom (respectively, 128-atom) supercells with a Brillouin zone sampling of 125 k points (respectively, 27 k points). The ion relaxation was performed using the standard conjugate-gradient algorithms implemented in the VASP code. More details on the method and in particular a comparison of full relaxation versus constant volume calculations for point defects in Fe can be found in Ref. 19. In all the tables presented below, the "number of atoms" is more precisely the number of Fe sites in the perfect supercell, i.e., the cell containing no defect.

The reference structure is the body-centered cubic structure with the lattice parameter obtained for pure Fe (2.8544 Å). The local magnetic moments have been used to describe the modification of the polarization of the electronic density which depends on the chemical interactions and on the relaxation of the structure induced by the presence of phosphorus and point defects. In order to calculate these local magnetic moments, it is necessary to introduce atomic radii to proceed to local projections (in the direct space of the electronic charge density) on spheres centerd on the atomic positions. The values adopted throughout this work are the recommended ones for the pseudopotentials used in the VASP code: 1.302 Å for Fe, 1.233 Å for P.

Except when otherwise mentioned, the defect formation energies are given taking as references the P atom in substitution as well as bcc α iron following in this the definitions of Ackland and coworkers.[14]

The formation enthalpy of a P atom in a supercell containing N sites is defined as the following when the P atom is in substitutional position:

$$E_{\text{for}}(\text{subs}) = E[(N-1)\text{Fe} + \text{P}] - (N-1)E[\text{Fe}] - E[\text{P}] \qquad (2.1)$$

and when the P atom is in interstitial position

$$E_{\text{for}}(\text{int}) = E[N\text{Fe} + \text{P}] - NE[\text{Fe}] - E[\text{P}]. \qquad (2.2)$$

$E[\text{P}]$ is the reference energy of a P atom. If one chooses the isolated P atom as reference, $E_{\text{for}}(\text{subs}) = -4.529$ eV for 54 atoms and $E_{\text{for}}(\text{subs}) = -4.463$ eV for 128 atoms. When the reference is P in substituted position, $E_{\text{for}}(\text{subs}) = 0$ eV.

The total binding energy between n defects, i.e., vacancies, self-interstitial atoms, or P atoms, is the energy difference between the configuration where all the defects interact and the system where all the defects are far from each other in order not to interact. Due to our limited supercell size and in order to subtract supercell energies obtained with the same cutoff and k points mesh, the total binding energy is calculated as

$$E_b(A_1,A_2,\cdots,A_n) = \sum_{i=1,n} E(A_i) - [E(A_1+A_2+\cdots+A_n) + (n-1)E_{\text{ref}}], \quad (2.3)$$

where E_{ref} is the energy of the supercell without any A_i, $E(A_i)$ is the energy of the supercell with A_i, and $E(A_1+A_2+\cdots+A_n)$ is the energy of the cell containing all A_i defects interacting. All the supercells contain the same number of sites, i.e., have the same size.

Another way of looking at these binding energies is in terms of reacting elements as considered for example in rate theory

$$A_1+A_2+\cdots+A_n \rightarrow [A_1+A_2+\cdots+A_n]. \quad (2.4)$$

This is specially useful when a rearrangement occurs (for instance when a solute atom in substitution jumps to form a mixed dumbbell).

III. SINGLE PHOSPHORUS IN BCC FE

A. Pure elements

Bulk properties obtained with VASP for pure iron have been investigated in details in our previous work[19] or in Ref. 35. At 0 K, our calculations are consistent with the experimental results. The ground state of Fe is magnetic bcc with an equilibrium lattice parameter of 2.8544 Å and a mean magnetic moment of 2.32 μ_B/at. As observed by Kresse and Joubert,[36] the magnetization is overestimated by 0.1 μ_B/at. compared to the experimental results.[37] The local magnetic moment after projection of the electronic density on the sphere centered on the atom (which radius is the radius used for local density of state projection) is 2.37 μ_B/at. The slight difference between the mean magnetic moment and the local magnetic moment comes probably from the overlap of the spheres.

Phosphorus solid phases have rather complex structures. Among the different known structures, the one formed by P_4 clusters is often encountered at low temperature.[38] We have checked that the isolated P_4 tetrahedron cluster is very stable (compared to other solid phases such as diamond), with a formation energy of −3.4 eV per P atom, the isolated P being our reference. The P-P equilibrium distance is 2.2 Å.

B. Single phosphorus in bcc Fe

Solute atoms can occupy substitutional or interstitial sites. The different interstitial configurations investigated here are mixed ⟨100⟩, ⟨110⟩, ⟨111⟩ dumbbells, octahedral, or tetrahedral sites [configurations $\langle 100\rangle_{\text{Fe-P}}$, $\langle 110\rangle_{\text{Fe-P}}$, $\langle 111\rangle_{\text{Fe-P}}$, (O), and (T)].

In agreement with experiment and the simulation results of Vasiliev and coworkers[13] the most stable position, and by far, for a P atom is on a crystallographic site, i.e., in substitution (configuration P_{subs} in Fig. 1). A large formation energy difference of about 3 eV is found for this configuration compared to all the interstitial positions investigated in Table I. Among the later, the mixed $\langle 110\rangle_{\text{Fe-P}}$ dumbbell is the most stable, followed by the octahedral configuration.

These interstitial configurations having close formation energies, a low activation energy for the migration of a P atom via interstitial sites may be expected leading thus to a high diffusion coefficient.

The experimental phosphorus diffusion coefficient in Fe, $1.38\times10^5 \exp(-3.4\ \text{eV}/kT)\ \text{cm}^2/\text{s}$ (in the temperature range 932–1017 K) and $8\times10^5 \exp(-3.2\ \text{eV}/kT)\ \text{cm}^2/\text{s}$ (in the temperature range 783–923 K)[9] is much larger than the self-diffusion coefficient. Indeed, at 870 K, the self-diffusion coefficient is $10^{-20}\ \text{m}^2/\text{s}$ (Mehrer, Stolica, and Stolwijk, p. 73)[39] while the diffusion coefficient of P in ferromagnetic bcc Fe is $10^{-17}\ \text{m}^2/\text{s}$ (Le Claire and Neumann, p. 179).[9] This fact could be associated with diffusion involving interstitials rather than vacancies.

In addition, if one supposes that migration takes place through some interstitial mechanism, the experimental activation energy of 3.2 eV (Ref. 9) can be decomposed into the P interstitial formation energy (close to 3 eV according to our calculations, Table I) and a migration energy which would thus be close to a few tenth of an electron volt (according to the value obtained for the interstitial formation energy). Such a migration energy is about the right order of magnitude for interstitial migration energies, and is in agreement with the closeness in energy of the various interstitial configurations.

The calculations done using a 16-atom supercell can only give a rough estimate of the energy of the substitutional configuration, despite the fact that the relaxation of the neighboring Fe atoms is rather small as will be seen later. For the interstitial configurations, the results are clearly not converged with 16 atoms, while going from 54 to 128 atoms leads to a reasonable convergence. For this reason, 54-atom supercells were used to investigate the different migration paths exposed in what follows.

Based on the data of Table I, the interaction of a migrating self-interstitial atom [the most stable one being the $\langle 110\rangle_{\text{Fe-Fe}}$ with a formation energy of 3.94 eV (Ref. 19)] with a substitute phosphorus atom can be estimated. The 2.98 eV formation energy for the $\langle 110\rangle_{\text{Fe-P}}$ compared to the 3.94 eV formation energy of the self-interstitial atom $\langle 110\rangle_{\text{Fe-Fe}}$ leads to a reaction energy between a P atom and the self-interstitial $\langle 110\rangle_{\text{Fe-Fe}}$ dumbbell of 0.96 eV. When a moving self-interstitial atom comes close to a phosphorus atom, the formation of a mixed dumbbell is very favorable. Under irradiation, numerous self-interstitial atoms which diffuse very rapidly are introduced in the materials. In the presence of P, our results indicate that mixed dumbbells may form in agreement with experiments. The formation and motion of mixed P dumbbells, thermally unstable, was indeed concluded by Abe and Kuramoto[40] out of their results from electrical resistivity recovery measurements on Fe-P dilute alloys irradi-

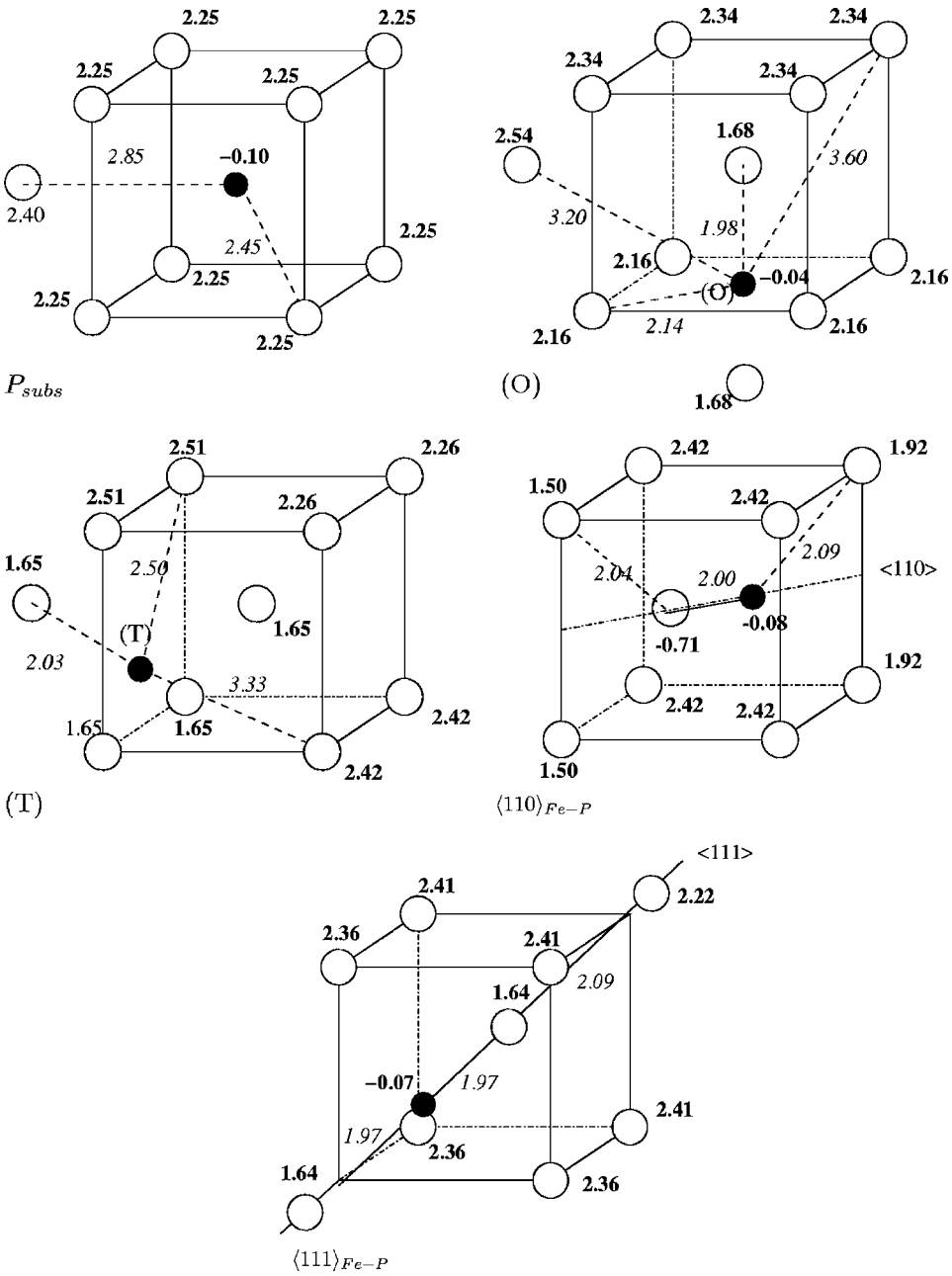

FIG. 1. Substitutional, octahedral (O), tetrahedral (T), and mixed dumbbells $\langle 100\rangle_{\text{Fe-P}}$, $\langle 110\rangle_{\text{Fe-P}}$, and $\langle 111\rangle_{\text{Fe-P}}$) P configurations. The relaxed distances (italic fonts) around the P atom are indicated in angstroms and the local magnetic moments (bold fonts) in Bohr magnetron. The reference lattice parameter a for Fe is 2.8544 Å and the local bcc Fe local magnetic moment is 2.37 μ_B. The phosphorus atom is the small black atom.

ated with 2.5 MeV electrons at 77 K. These interactions between P and interstitial atom will be presented in more detail in Sec. V.

The relaxation of the nearest neighbor Fe shells around a P in substitutional position is −0.9%, −0.03%, and −0.2% for the first, second, and third nearest Fe atom shells. These results are expressed in terms of $\Delta d_i/d_i^0$, where d_i^0 is the distance between the impurity and the atom before any relaxation, d_i is the new distance between the impurity and the atom after the relaxation, and i is the index of the neighbor shell. This relaxation is thus inward and small (below 1%), indicating that the P atom is slightly undersized as compared to the Fe atom in agreement with King's[26] data.

The distances after relaxation between the Fe atom and the P atom are represented Fig. 1 along with the local magnetic moments carried by each atom.

IV. PHOSPHORUS–VACANCY INTERACTION

A. Interaction energy

The interaction of one P atom with a single vacancy has been evaluated when the two defects are first, second, and up to fifth nearest neighbors (Table II). In first and second nearest positions (1nn and 2nn) the binding energy is positive (indicating attraction) and large (between 0.25 and 0.3 eV) while at larger distance it vanishes indicating that no more interaction between the vacancy and the phosphorus atom exists. These results are partly in agreement with those of Vasiliev and coworkers[13] who find a strong binding energy between the vacancy and the P atom of 0.39 eV but in second nearest neighbor position only. Our results are in agreement with the binding energy calculated by Ackland *et al.* on small supercells.[18]

TABLE I. Formation enthalpy E_{for} (in electron volts) for different positions of the P atom in the Fe matrix. For P, the reference state is the atom in substitution in the bcc lattice, for Fe, bcc Fe. The calculations were done using 54 atom supercells and 125 k points as well as with 128 atom supercells with 27 k points. The Ackland *et al.* (Ref. 18) *ab initio* calculations have been obtained with 16 atom supercells whereas the EAM results are for 2000 atoms.

Configuration	EAM[a]	P (16 at.)[a]	P (16 at.)	P (54 at.)	P (128 at.)
P_{subs}	0	0	0	0	0
(T)	2.80	4.35	4.35	3.236	
(O)	3.47		4.75	3.135	2.973
$\langle 100\rangle_{Fe\text{-}P}$	Decays to mixed $\langle 110\rangle$	4.75		Decays to (O)	Decays to (O)
$\langle 110\rangle_{Fe\text{-}P}$	2.57	3.82	3.83	2.98	2.924
$\langle 111\rangle_{Fe\text{-}P}$	3.30	4.36	4.35	3.403	3.25

[a]Reference 18.

P is known to segregate at free surfaces, and as a vacancy can be considered as the first step toward the creation of a surface, a positive binding energy is not surprising. However such a large binding energy (0.31 eV) was not expected and thus not taken into account in the models built until now.[6] Note however that in austenitic steels, it was observed that the presence of P atoms suppresses the segregation of Ni atoms to voids and the results were interpreted as P-vacancies (P-V) interactions.[41]

The P atom relaxes towards the vacancy, the V-P distance is 2.37 Å, whereas the nearest neighbor distance in bcc Fe is 2.47 Å. The relaxation of a phosphorus atom first nearest neighbor to a vacancy is similar to that of an Fe atom first neighbor to a vacancy (the V-Fe distance is 2.36 Å).[19]

This indicates thus that the large binding energy is mainly due to chemical rather than elastic effects.

The migration energy of a P atom toward a vacancy has been obtained by placing the P atom halfway between the two nearest neighbor sites occupied by the P and the vacancy. The structure is relaxed using the conjugate gradient algorithm and the energy of the new configuration is determined.

By looking at the vibrational modes of the P atom, it was verified that this position is indeed a saddle point and not a local minimum, and the migration energy is the energy difference between the relaxed initial configuration (where the P atom is in substitution and the vacancy in first nearest neighbor position to the P atom) and the energy of the halfway position. The value thus obtained equals 0.337 eV (Table II). A large and positive binding energy between a P atom and one vacancy associated with a P low migration energy indicates that the formation of V-P pairs is very plausible, in which the vacancy can exchange easily with the P atom. The EAM potential developed by Ackland *et al.*[18] also predicts a low migration energy of 0.31 eV.

These results being a bit unexpected, a sensitivity study of the values obtained for the binding and migration energies to the *ab initio* method used was performed. Taking into account the Vosko *et al.* corrections[33] with USPP leads to a binding energy of 0.24 eV for both positions of the vacancy (i.e., first and second neighbor to the P atom), and does not change the migration energy. The use of PAW instead of ultrasoft pseudopotentials does not affect significantly our results either.

B. P diffusion coefficient

The experimental diffusion coefficient of P in bcc Fe is one to two orders of magnitude larger than the Fe self diffusion coefficient.[9] According to Le Claire,[42] impurities diffuse by the vacancy mechanism when their diffusion rates are comparable with the host self diffusion rate. When the impurity diffusion rate greatly exceeds that of self diffusion, the vacancy mechanism is untenable and diffusion is believed to be dominated by some form of interstitial migration. P is one example for which diffusion via interstitials could be assumed.

Because of the large V-P binding energy and the low P migration energy obtained in our calculations, the diffusion

TABLE II. P-V binding energies (in electron volts) and P migration energy (in electron volts). The calculations were done using 54 atom supercells and 125 k points.

Configuration	EAM[a]	USPP (54 at.)	USPP+Vosko[b] (54 at.)	PAW (54 at.)	USPP (128 at.)
V-P 1nn	0.37	0.31	0.24	0.35	0.32
V-P 2nn	0.34	0.26	0.24	0.22	0.28
V-P 3nn	−0.07	−0.02			−0.03
V-P 4nn	−0.03	−0.05			−0.01
V-P 5nn	−0.02	−0.04			
P migration	0.31	0.34	0.34	0.41	0.34

[a]Reference 18.
[b]Reference 33.

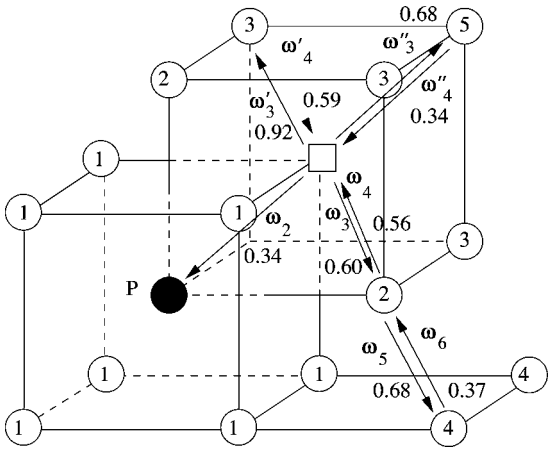

FIG. 2. Definition of the different jumps w_i of the vacancy (square) with a solute atom (black circle) and corresponding migration energies E_i^{mig}. The number in the circles indicates the relative position of the site to the solute atom, 1 meaning first nearest neighbor of the solute… [from Philibert (Ref. 42)].

coefficient for migration via a vacancy mechanism was determined.

If one assumes a vacancy mechanism for the migration of P in Fe, the diffusion coefficient can be obtained using the nine-frequency model developed by Le Claire[43] for heterodiffusion in bcc crystal. This method has been previously applied for Cu in Fe using empirical potential[44] as well as *ab initio* results.[45]

The different possible jumps involved in the diffusion assuming only first and second nearest neighbor interactions, defined in Fig. 2, have thus been evaluated. It is noteworthy that in this situation, as in the two cases cited above, the common simplified models based on only first nearest neighbor or only second nearest neighbor interactions cannot be applied as neither first or second nearest neighbor P-vacancy interaction can be neglected.

In Fig. 2 the classical jump frequency notation has been adopted, see, e.g., the Philibert book.[46] When positioned in a first nearest neighbor position, the vacancy can go away from the P atom by jumps in second (jump with frequency w_3 in Fig. 2), third (frequency w_3') or fifth (frequency w_3'') nearest neighbor positions.

As the binding energy between the vacancy and the phosphorus atom in second nearest neighbor position is large, the jump from second to fourth nearest neighbor position (jump with frequency w_5 in Fig. 2) has to be considered also. All other vacancy jumps are equivalent to the vacancy jumps in pure Fe, which was found to have a migration barrier of 0.65 eV,[19] assuming, in agreement with our calculations (Table II), that there is no interaction between the P atom and the vacancy after the third nearest neighbor shell. The different migration paths have been determined with a 54-atom supercell and 125 k points. To find the saddle point position for each jump, a set of configurations has been built going from the initial to the final relaxed positions. For each intermediate position, the migrating atom has been constrained to remain within a (100) plane. This method prevents the moving atom from falling in the minimum energy structure and allows thus the determination of the activation barrier.

The energy differences between the saddle point position and the initial and final configurations give the migration energies for the jumps in the two directions.

These energies are summarized in Table III and have been used to determine the P diffusion coefficient. The Ackland *et al.* EAM potential predicts migration energies whose difference with our *ab initio* calculations is lower than 0.1 eV (except for the jump between first and fifth nearest neighbor position). In agreement with the large V-P binding energy, the jumps toward the vacancy are always easier than the jumps away from it.

To evaluate diffusion coefficients of a solute in a matrix element, a common approximation is made which consists in considering that the attempt frequencies are all equal. This can be acceptable for atoms with similar atomic mass and size. However, as Fe and P are quite different in terms of bonding and mass, the attempt frequency has been evaluated in the framework of the Vineyard transition state theory.[47] In this model, $\nu_i = \Pi_1^{3N} \tilde{\nu}_j / \Pi_1^{3N-1} \tilde{\nu}_j^*$. $\tilde{\nu}_j$ are the vibration modes in the initial configuration and $\tilde{\nu}_j^*$ the vibrational modes in the transition state configuration N is the number of atoms.

Within the Einstein approximation, only the vibrational modes of the migrating atom have to be considered. Compared to other approximations made in the model, this should provide a good order of magnitude. The three vibrational modes of a P atom in an equilibrium first nearest neighbor position to a vacancy, and the two positive modes at the relaxed saddle point have been obtained by moving the P atom by 0.05 Å along each direction. The same procedure has been applied to a Fe atom in Fe.

The attempt frequencies calculated this way are ν_{Fe} equals 4.9 THz for the Fe atom and ν_{P} equals 3.8 THz for the P atom. It is interesting to note that despite the differences in

TABLE III. Migration energies (electron volts) corresponding to the different jumps represented Fig. 2. Calculations done in 54-atom supercells with 125 k points.

Jump A—B	A→B	B→A	A→B EAM[a]	B→A EAM[a]
1nn—1nn	0.34 (w_2)	0.34 (w_2)	0.31	0.31
1nn—2nn	0.60 (w_3)	0.56 (w_4)	0.64	0.62
1nn—3nn	0.92 (w_3')	0.59 (w_4')	1.04	0.62
1nn—5nn	0.68 (w_3'')	0.34 (w_4'')	0.90	0.51
2nn—4nn	0.68 (w_5)	0.37 (w_6)	0.67	0.30

[a]Reference 18.

mass and chemistry between the P and the Fe atoms, their attempt frequencies are rather close.

The jump frequency of a vacancy w_i or w_i' to a neighboring site is given by

$$w_i = \nu_i \exp - \frac{E_i^{\mathrm{mig}}}{kT}. \tag{4.1}$$

The self-diffusion coefficient is[46]

$$D_{\mathrm{Fe}} = a^2 w_0 f_0 c_v^{\mathrm{eq}}, \tag{4.2}$$

where f_0 is the self-diffusion correlation factor (0.727 for bcc), and c_v^{eq} is the equilibrium vacancy concentration at temperature T. The solute P diffusion coefficient equals[43]

$$D_P = a^2 w_2 f_2 \frac{w_4'}{w_3'} c_v^{\mathrm{eq}}. \tag{4.3}$$

Taking into account the different jumps described in Fig. 2, and assuming that all the other jumps are not affected by the presence of P and have frequency w_0, the impurity correlation factor f_2 is given by[43]

$$f_2 = \frac{1+t_1}{1-t_1} \tag{4.4}$$

and[43]

$$t_1 = - \frac{w_2}{w_2 + 3w_3 + 3w_3' + w_3'' - \dfrac{w_3 w_4}{w_4 + F w_5} - \dfrac{2 w_3' w_4'}{w_4' + 3 F w_0} - \dfrac{w_3'' w_4''}{w_4'' + 7 F w_0}} \tag{4.5}$$

with $F=0.512$.

In this calculation, we assumed that all the attempt frequencies ν_i for P (for the jumps w_0, w_3, w_3', w_3'', w_4, w_4', and w_5) were similar and taken equal to ν_{Fe}.

The vacancy formation energy was taken to be 2.02 eV.[19] After determining D_P for different temperatures between 200 and 1000 K, and fitting these data by an exponential law, we obtain: $D_P = 4.48 \times 10^{-3} \exp(-2.30\ \mathrm{eV}/kT)\ \mathrm{cm}^2/\mathrm{s}$ and $D_{\mathrm{Fe}} = 2.95 \times 10^{-3} \exp(-2.66\ \mathrm{eV}/kT)\ \mathrm{cm}^2/\mathrm{s}$.

According to our calculations, the diffusion coefficient of P based on a vacancy mechanism is thus larger than the self-diffusion coefficient by one to three orders of magnitude as can be seen Fig. 3. These values are however lower (see Fig. 3), than the experimental values for the diffusion coefficient of P in bcc Fe.

Our results confronted with the experimental data indicate thus that despite the high P vacancy binding energy, diffusion based on interstitial mechanisms is more probable. This point will be further discussed in the discussion on phosphorus-interstitial interactions. Nevertheless, our calculations indicate also that P diffusion via a vacancy based mechanism should be much faster than self diffusion.

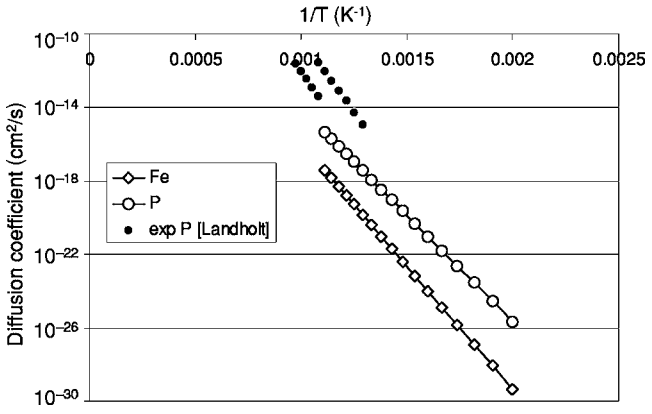

FIG. 3. P and self-diffusion coefficients versus inverse temperature. The experimental data are from Ref. 9.

C. Monte Carlo study of the motion of V-P pairs

The diffusivity of a V-P pair has been studied by atomistic kinetic Monte Carlo, using the migration energies determined with the nine jump model. The diffusion of a V-P pair has been investigated at different temperatures using the residence time algorithm.[48]

A kinetic Monte Carlo step consists in choosing one of the eight possible vacancy jumps for a configuration according to their occurrence frequency Γ_k (equals w_i, w_i', or w_i'' depending on the relative position of the vacancy to the phosphorus atom). The average time step associated to the kinetic Monte Carlo step is

$$dt = \frac{1}{\sum_{k=1,8} \Gamma_k}. \tag{4.6}$$

The simulation of the pair (initially introduced in first nearest neighbor position) was kept track of until its dissociation or up to 10^6 kinetic Monte Carlo steps. The lifetime of the pair, as well as its mean free path $\langle R_P^2 \rangle$ before dissociation have been statistically determined using 100 000 simulations per temperature.

Plots of the P-V pair mean free paths for three temperatures (until the pair dissociation, the critical distance chosen being 6.4 Å) are shown Fig. 4. For all the temperatures investigated, the mean free path of the P-V pair is small (Fig. 4). The distribution has a maximum around 5 Å. For each temperature, the mean lifetime distribution follows a Poisson

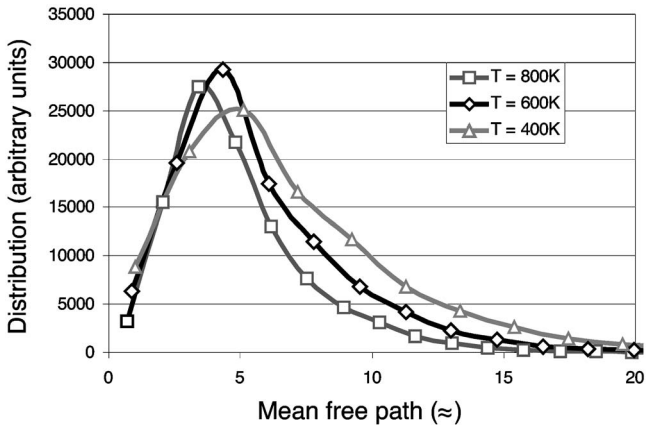

FIG. 4. P-V pair mean free path distribution for three different temperatures. (100 000 simulations).

law $\{\exp[-d/\tau(T)]\}$ and as expected the lifetime is longer for lower temperatures. We have determined τ for different temperatures between 400 and 1000 K. The interpolation of τ as a function of temperature leads to $\tau(T)=6\times10^{-13}\exp(0.66\ \mathrm{eV}/kT)$ (in s).

The vacancy jumps away from the P atom (w_3'', w_5) have an activation energy close to 0.7 eV, while it is the reverse jumps (w_4'' and w_6) which have a low activation energy (around 0.4 eV). The only jump inducing the migration of the P atom is the first nearest neighbor jump. In order for the atom to move further, the vacancy has to easily migrate between first and second nearest neighbor positions of the P atom. A low migration energy between the 1nn and 2nn positions compared to the migration energies of other jumps is thus required. The barrier of 0.60 eV is not low enough for this mechanism to proceed for a very long time.

In conclusion, the migration of P-V pairs does not lead to a large mean free path. The P-V pair has a mean lifetime given by $\tau(T)=6\times10^{-13}\exp(0.66\ \mathrm{eV}/kT)$ s. Our results indicate thus that despite a high P-V binding energy the migration of a P-V pair is not a very efficient mechanism to transport P atom.

V. PHOSPHORUS–SELF-INTERSTITIAL ATOM INTERACTIONS

As phosphorus diffusion is thought of as possibly taking place via some interstitial mechanisms, we carefully investigated the different interactions a P atom can establish with a self interstitial.

A. Single P atom—self-interstitial atom interactions

The most stable self interstitial in Fe is the $\langle110\rangle_{\text{Fe-Fe}}$ dumbbell (Fig. 5).

The dumbbell migration process was thought by Johnson[49] to occur by either a simple jump of one of the atoms constituting of the dumbbell and the recently formed dumbbell belongs thus to the same (110) plane as the old dumbbell or by a jump followed by a rotation. In that later case, the new dumbbell changes (110) plane. Recent *ab initio*

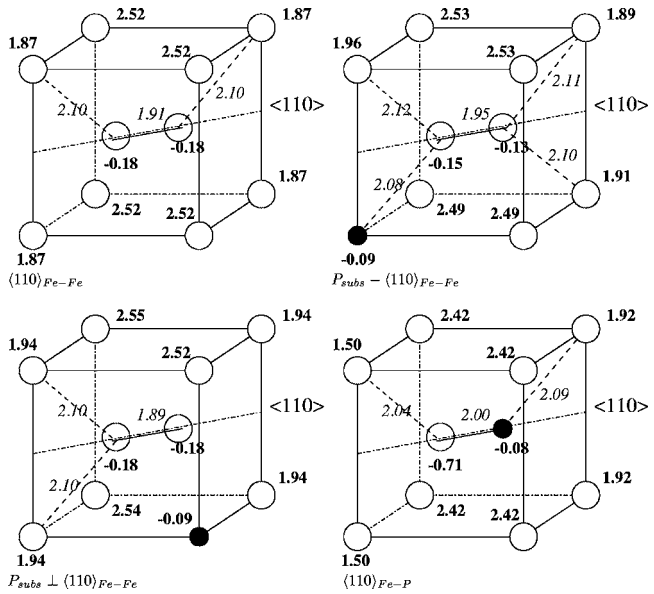

FIG. 5. The self-interstitial $\langle110\rangle_{\text{Fe-Fe}}$ dumbbell and the three different positions for a P atom interacting with it. The fourth figure corresponds to the mixed $\langle110\rangle_{\text{Fe-P}}$ dumbbell. The relaxed distances (italic fonts) around the P atom are indicated in angstroms and the local magnetic moments (bold fonts) in Bohr magnetron. The reference lattice parameter a for Fe is 2.8544 Å and the local magnetic moment of the Fe atom in the bcc structure is 2.37 μ_B. The phosphorus atom is the small black atom.

calculations[50] have shown that the most favorable mechanism was the jump followed by a rotation.

The binding (or reaction) energy of the $\langle110\rangle_{\text{Fe-Fe}}$ dumbbell with a P atom positioned on a regular crystallographic site has been determined for the three different final configurations represented in Fig. 5, and the values obtained are reported in Table IV.

When a P atom moves to become part of a mixed dumbbell (configuration $\langle110\rangle_{\text{Fe-P}}$) the total reaction energy is close to 1 eV (0.96 eV for a 54-atom supercell and 1.02 eV for a 128-atom supercell). It is close to 0.84 eV when the P atom remains in first nearest neighbor position in the (110) plane containing the dumbbell (configuration $P_{\text{subs}}-\langle110\rangle_{\text{Fe-Fe}}$).

The strong interaction between the self interstitial $\langle110\rangle_{\text{Fe-Fe}}$ dumbbell and the substitutional P atom, was also analyzed in terms of formation energies in the first section of this paper.

When the final configuration is $P_{\text{subs}}\perp\langle110\rangle_{\text{Fe-Fe}}$ where the P atom is first neighbor to the dumbbell but not in the (110) plane containing it, a repulsion close to 0.36 eV is observed. The large affinity of P for configurations $P_{\text{subs}}-\langle110\rangle_{\text{Fe-Fe}}$ and $\langle110\rangle_{\text{Fe-P}}$ is in agreement with the smaller size of the P atom as compared to that of the Fe atom. Indeed the presence of the self-interstitial $\langle110\rangle_{\text{Fe-Fe}}$ dumbbell introduces a strain in the (110) plane defined by the dumbbell and its first four nearest neighbor Fe atoms. P being an undersized atom as previously established from the relaxation mode of its neighbor atoms, the strain induced by the dumbbell is reduced when a smaller atom is introduced in that plane.

TABLE IV. P-$\langle 110\rangle$ interstitial interactions. The binding energies (in electron volts) are given taking as references (or initial configurations for the reaction) the P atom in substitution and the self $\langle 110\rangle_{\text{Fe-Fe}}$. The values in parentheses are the formation energies, taking as references bcc Fe and P in substitution. The calculations were done using 54-atom supercells with 125 k points, and 128-atom supercells and 27 k points.

Final configuration	54 atoms	128 atoms
$\langle 110\rangle_{\text{Fe-P}}$	0.96 (3.00)	1.02 (2.92)
$P_{\text{subs}}-\langle 110\rangle_{\text{Fe-Fe}}$	0.85 (3.11)	0.83 (3.11)
$P_{\text{subs}}\perp\langle 110\rangle_{\text{Fe-Fe}}$	–0.36 (4.32)	–0.35 (4.29)

The repulsion observed for configuration $P_{\text{subs}}\perp\langle 110\rangle_{\text{Fe-Fe}}$ is also coherent with the fact that the P is on a site not situated in the (110) plane defined by the dumbbell and its first four nearest neighbor Fe atoms. This site is under dilation, and a "small" atom will prefer to sit on a substitutional site rather than on a site under dilation.

This affinity of undersized solutes with self interstitials was expected, but the "amount" of attraction depends on the elastic effects as well as on the chemical interactions, which are not *a priori* easy to forecast. This will for instance affect the mobilities of the solutes.

A priori the two possible jumps, with and without rotation of the dumbbell, are possible. However the repulsion observed for configuration $P_{\text{subs}}\perp\langle 110\rangle_{\text{Fe-Fe}}$ indicates that rotation without jump is reduced. On the other hand the large reaction energy obtained when forming the mixed dumbbell ($\langle 110\rangle_{\text{Fe-P}}$) and the large binding energy of configuration $P_{\text{subs}}-\langle 110\rangle_{\text{Fe-Fe}}$, where the P atom is first neighbor to the $\langle 110\rangle_{\text{Fe-Fe}}$ dumbbell indicate that these configurations are very likely and that diffusion of the P atom via these two configurations is very plausible. Indeed the typical path for the migration of the $\langle 110\rangle$ dumbbell[49,50] goes from one configuration $\langle 110\rangle_{\text{Fe-P}}$ to a configuration $P_{\text{subs}}-\langle 110\rangle_{\text{Fe-Fe}}$.

B. Two P in interstitial sites

When a mixed $\langle 110\rangle_{\text{P-Fe}}$ interstitial diffuses, it can encounter another P atom in a substitutional site position and form a di-interstitial. Depending on the stability of the di-interstitial formed, it can be more or less mobile, may lead to trapping of a self interstitial $\langle 110\rangle_{\text{Fe-Fe}}$, or to the diffusion of the complex formed.

Different configurations have thus been studied: the three kinds of P-P dumbbells as well as various configurations related to the eventual detrapping or migration of the di-interstitial. Among the three configurations possible for the P-P dumbbell, configuration $\langle 110\rangle_{\text{P-P}}$ is the most stable followed by configuration $\langle 100\rangle_{\text{P-P}}$ and $\langle 111\rangle_{\text{P-P}}$ (see Fig. 6 and Table V). Note that the mixed $\langle 100\rangle_{\text{P-Fe}}$ is not stable while the $\langle 100\rangle_{\text{P-P}}$ is more stable than the $\langle 111\rangle_{\text{P-P}}$.

The interaction of two P atoms and a self-interstitial $\langle 110\rangle_{\text{Fe-Fe}}$ dumbbell has been investigated in more detail. The different possible final configurations studied are represented in Fig. 7 (the notation takes into account which atom belongs to the (110) plane containing the dumbbell) and the corresponding reaction energies are gathered in Table V. Configuration $\langle 110\rangle_{\text{P-P}}$ is less stable than a mixed dumbbell close to a substitutional P atom, i.e., configuration $P_{\text{subs}}-\langle 110\rangle_{\text{Fe-P}}$. Configuration $P_{\text{subs}}-\langle 110\rangle_{\text{P-Fe}}$ is unstable and decays to $\langle 100\rangle_{\text{P-P}}$.

The most stable configuration is $P_{\text{subs}}-\langle 110\rangle_{\text{Fe-P}}$ with one P in mixed dumbbell configuration and the other one on the first nearest neighbor site to the Fe atom from the mixed dumbbell. The total binding energy is around 2.1 eV.

When a mixed $\langle 110\rangle_{\text{Fe-P}}$ dumbbell comes near a substitutional P atom following the reaction $P_{\text{subs}}+\langle 110\rangle_{\text{Fe-P}}\rightarrow P_{\text{subs}}-\langle 110\rangle_{\text{Fe-P}}$, the associated reaction energy (or binding energy) is 1.1 eV for a 128-atom supercell. Thus, the dissociation of the most stable configuration ($P_{\text{subs}}-\langle 110\rangle_{\text{Fe-P}}$) costs about 1 eV and is not very favorable. The dissociation of the two other configurations is not very favorable either and costs about 0.6 eV. The mixed dumbbell $\langle 110\rangle_{\text{Fe-P}}$ has thus been trapped by the other P atom and become sessile. These results may explain the increase of the self-interstitial effective migration energy which goes from 0.31 eV in pure Fe to 0.79 eV in $\text{FeP}_{0.11\%}$ as measured by Hardouin du Parc.[10] This situation can also be seen as the trapping of a pure $\langle 110\rangle_{\text{Fe-Fe}}$ dumbbell by two P atoms close together (initially located in second, third, or fifth nearest neighbor position to each other).

The objects composed of one pure Fe dumbbell ($\langle 110\rangle_{\text{Fe-Fe}}$) and two P atoms in substitutional position ($2P_{\text{subs}}-\langle 110\rangle_{\text{Fe-Fe}}$, $P_{\text{subs}}-\langle 110\rangle_{\text{Fe-Fe}}-P_{\text{subs}}$), have also high binding energies close to 1.7 eV. This can also indicate a trapping effect of the dumbbell by two P atoms.

The configuration $P_{\text{subs}}-\langle 110\rangle_{\text{P-Fe}}$ where the two P atoms are first nearest neighbors is unstable, P atoms prefer thus not to be in first nearest neighbor positions.

In order to evaluate the potential dissolution of the configurations previously explored, the relative stability of a cluster of an interstitial and two phosphorus atoms has been compared with some configurations derived from the most stable configurations, namely, configuration $P_{\text{subs}}-\langle 110\rangle_{\text{Fe-P}}$ and configuration $2P_{\text{subs}}-\langle 110\rangle_{\text{Fe-Fe}}$. These configurations (Fig. 8) result from the migration of one atom out of the dumbbell (mixed or not) to form another dumbbell (mixed). The corresponding reactions are

$$2P_{\text{subs}}-\langle 110\rangle_{\text{Fe-Fe}}\rightarrow P_{\text{subs}}-a(001)-\langle 110\rangle_{\text{P-Fe}} \quad (5.1)$$

$$P_{\text{subs}}-\langle 110\rangle_{\text{Fe-P}}\rightarrow P_{\text{subs}}-a\sqrt{2}(110)-\langle 110\rangle_{\text{P-Fe}} \quad (5.2)$$

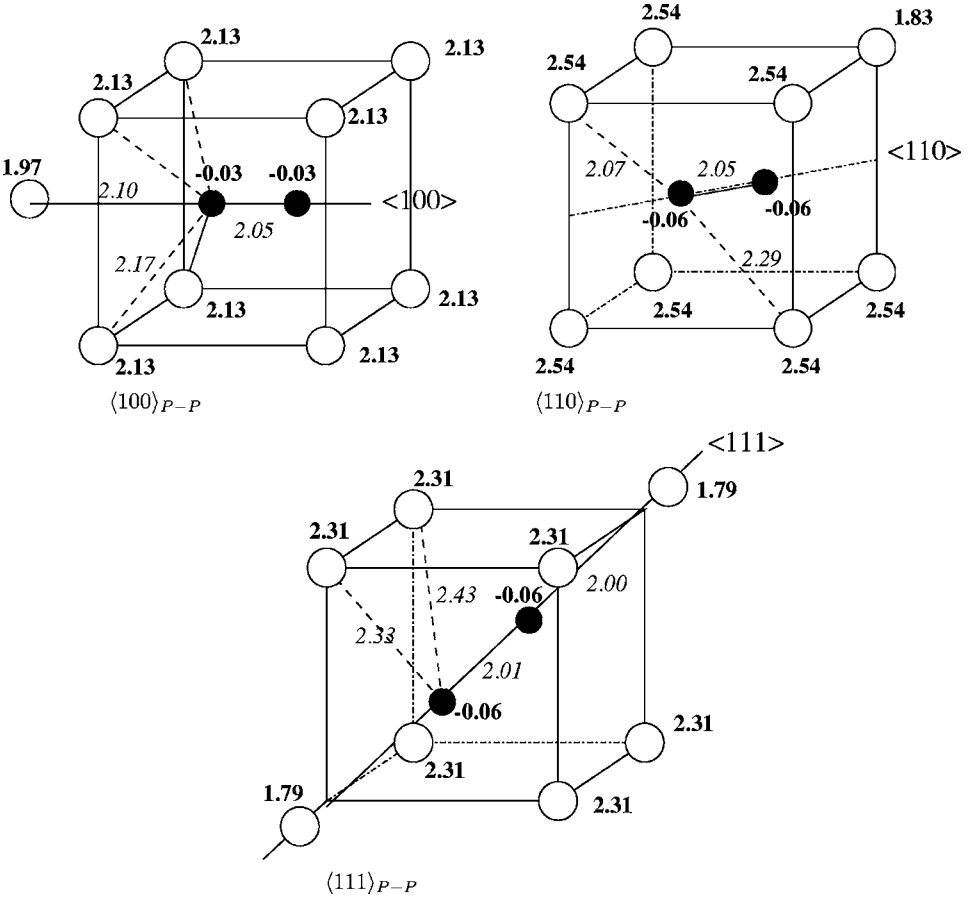

FIG. 6. Structure of three P atoms both in interstitial positions: $\langle 100\rangle_{\text{P-P}}$ $\langle 110\rangle_{\text{P-P}}$ and $\langle 111\rangle_{\text{P-P}}$ and the local magnetic moments (bold fonts) in Bohr magnetron. The reference lattice parameter a for Fe is 2.8544 Å and the local magnetic moment of the Fe atoms in the bcc structure is 2.37 μ_B. The phosphorus atoms are the small black atoms (54 atoms and 125 k points).

$$P_{\text{subs}} - \langle 110\rangle_{\text{Fe-P}} \rightarrow P_{\text{subs}} - a\sqrt{3}(111) - \langle 110\rangle_{\text{P-Fe}} \quad (5.3)$$

Table V indicates that these configurations are much less stable than the configurations they come from. The binding energies of these three configurations are lower and close to the binding energy of only one P atom with an interstitial (Table IV). The interaction with the second P atom in these configurations is thus not effective.

Consequently, in a solid solution containing some P atoms, self-interstitial atoms will tend to form mixed dumbbells which can migrate and transport P. However, these mixed dumbbells appear to be easily trapped by other P atoms in the matrix, and the effective diffusion coefficient of interstitials may be reduced consequently.

VI. SUBSTITUTIONAL P-P INTERACTION

The binding energy of two P atoms both in substitutional position is negative indicating repulsion as can be seen in Table VI. This repulsion is larger when the P atoms are first

TABLE V. P—$\langle 110\rangle_{\text{Fe-P}}$ reactions. The reaction (or binding) energies (in electron volts) are given taking as references (or initial configuration) both P atoms in a substitutional site (noninteracting with each other) and the self-interstitial atom ($\langle 110\rangle_{\text{Fe-Fe}}$). The final configurations are shown Figs. 6–8. The values in parenthesis are the formation energies taking as references bcc Fe and P in substitution. The calculations were done in 54-atom supercells and 125 k points as well as 128-atom supercells with 27 k points.

Final configuration	d(P-P) (Å)	54 atoms	128 atoms
$\langle 110\rangle_{\text{P-P}}$	2.05	1.29 (2.67)	1.42 (2.52)
$P_{\text{subs}}-\langle 110\rangle_{\text{Fe-P}}$	3.27	2.04 (1.92)	2.12 (1.83)
$P_{\text{subs}}-\langle 110\rangle_{\text{P-Fe}}$		Decays to $\langle 100\rangle_{\text{P-P}}$	Decays to $\langle 100\rangle_{\text{P-P}}$
$2P_{\text{subs}}-\langle 110\rangle_{\text{Fe-Fe}}$	3.59	1.59 (2.37)	1.65 (2.29)
$P_{\text{subs}}-\langle 110\rangle_{\text{Fe-Fe}}-P_{\text{subs}}$	4.57	1.69 (2.27)	1.67 (2.27)
$\langle 100\rangle_{\text{P-P}}$	2.05	0.89 (3.07)	
$\langle 111\rangle_{\text{P-P}}$	2.01	0.46 (3.50)	
$P_{\text{subs}}-a(001)-\langle 110\rangle_{\text{P-Fe}}$	3.18	0.91 (3.05)	0.99 (2.95)
$P_{\text{subs}}-a\sqrt{2}(110)-\langle 110\rangle_{\text{P-Fe}}$	3.35	0.90 (3.06)	0.98 (2.96)
$P_{\text{subs}}-a\sqrt{3}(111)-\langle 110\rangle_{\text{P-Fe}}$	3.80	1.09 (2.87)	1.16 (2.78)

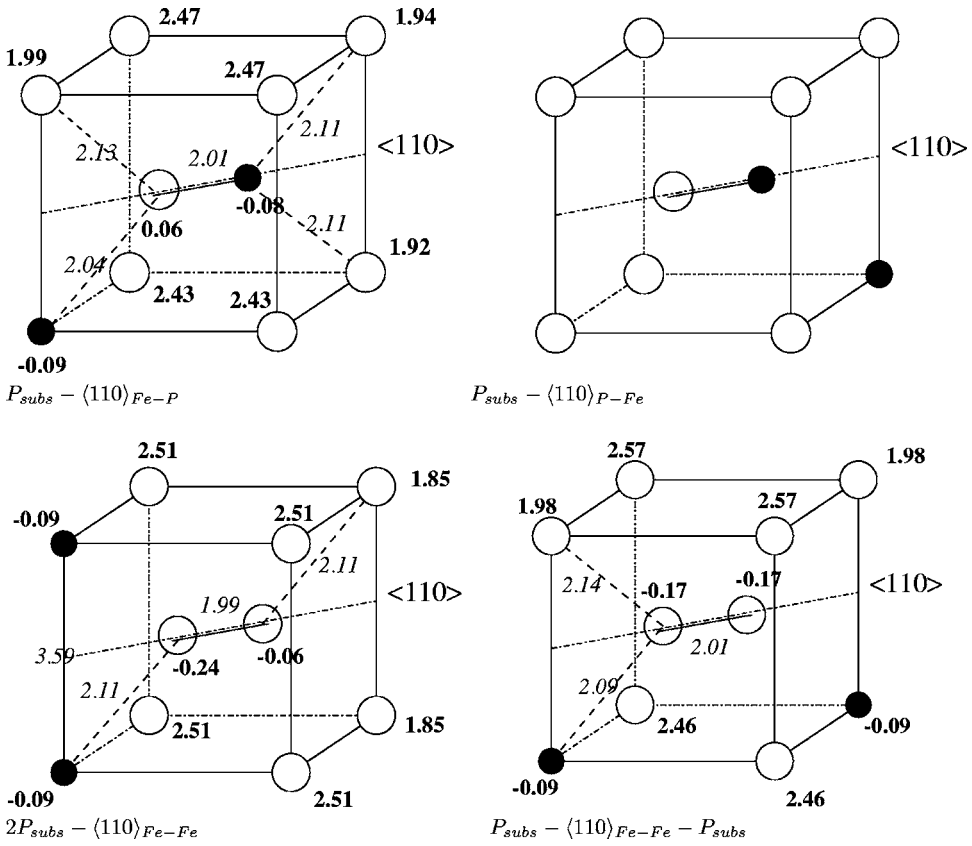

FIG. 7. Final configurations after the reaction of two P atom and a $\langle 110 \rangle_{\text{Fe-Fe}}$ dumbbell. The notation takes into account which atom belongs to the (110) plane containing the dumbbell. The relaxed distances (italic fonts) around the P atom are indicated in angstroms and the local magnetic moments (bold fonts) in Bohr magnetron. The reference lattice parameter a for Fe is 2.8544 Å and the local magnetic moment for the Fe atom in the bcc structure is 2.37 μ_B. The phosphorus atoms are the small black atoms (54 atoms and 125 k points).

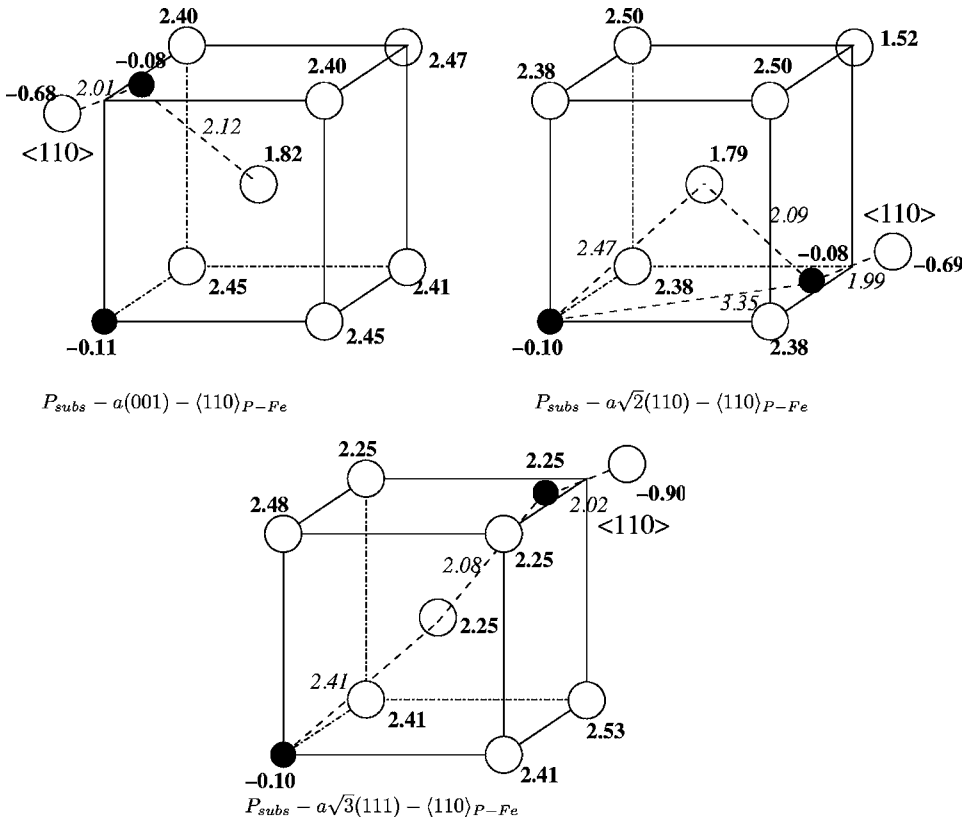

FIG. 8. Possible intermediate configuration to dissociation of some of the most stable complexes. The relaxed distances (italic fonts) around the P atom are indicated in angstroms and the local magnetic moments (bold fonts) in Bohr magnetron. The reference lattice parameter a for Fe is 2.8544 Å and the local magnetic moment of the Fe atoms in the bcc structure is 2.37 μ_B. The phosphorus atoms are the small black atoms (54 atoms and 125 k points).

TABLE VI. P-P binding energies (in electron volts) when both P atoms are on substitutional sites. The calculations were done using 54-atom supercells with 125 *k* points. The lattice site distance between the P atoms is given in terms of the lattice parameter of Fe: 2.8544 Å.

Configuration	d(P-P) (a_0)	54 atoms	128 atoms
P-P 1nn	$\sqrt{3}/2$	−0.172	−0.17
P-P 2nn	1	−0.108	−0.06
P-P 3nn	$\sqrt{2}$	−0.026	−0.01

neighbors than when they are second neighbors. It vanishes when they are third or higher neighbors.

Nevertheless, P-P pairs may form when a mixed dumbbell diffusing meets with a vacancy-phosphorus defect. Indeed both defects were found to be able to form easily specially in an irradiated environment. However because of the repulsion induced by the two P atoms, the P atoms will remain further away from each other than first or second neighbours.

Thus, successive interactions of P atoms with point defects may lead to the formation of P rich clusters, however dilute ones. This may be an explanation for the formation of the dilute P clusters observed by atom probe experiments.[3]

VII. CONCLUSIONS

To investigate the diffusion of P in bcc iron, we have determined its interaction with point defects in the framework of the density functional theory. P favors being in substitutional position whereas the mixed ⟨110⟩ dumbbell is the most favourable interstitial configuration.

For both vacancies and interstitials a strong binding or reaction energy is obtained leading to the formation of P-V pairs or mixed $\langle 110\rangle_{\text{Fe-P}}$ dumbbells, indicating a large interaction of phosphorus atoms with intrinsic point defects in the α Fe matrix. These results have consequences on the diffusivity properties of phosphorus. More precisely:

(1) The binding energy between a P atom and a vacancy is large in first and second nearest neighbor positions whereas the P migration energy by exchange with a vacancy is very low (0.3 eV) compared to Fe migration energy (0.65 eV). This low migration energy coupled with the strong *V*-P binding energies can lead to the formation of stable V-P pairs. The analysis of the diffusivity properties of the P-V pairs however indicates that the pairs have a small mean free path.

(2) P interacts strongly with ⟨110⟩ self-interstitial atoms. The formation of a mixed dumbbell out of a self-interstitial Fe atom and a P atom in substitution leads to an energy gain of 0.96 eV. Thus under irradiation, self interstitial Fe atoms migrating in the Fe matrix may be attracted by substitutional P atoms to form mixed $\langle 110\rangle_{\text{Fe-P}}$ dumbbells which can then migrate. However, these mixed dumbbells appear to be easily trapped by other P atoms in the matrix, and the effective diffusion coefficient of interstitials may be reduced consequently. In a similar way, the interaction of two phosphorus atoms with a ⟨110⟩ self-interstitial atom may also lead to some stable and *a priori* sessile configurations.

(3) Two P atoms both in substitutional positions in first and second nearest neighbor positions repel each other. This repulsion may prevent the formation of pure P clusters, and can explain the experimental observation by tomographic atom probe of the formation under neutron irradiation of dilute phosphorus clusters.

The data obtained by *ab initio* calculations gives insight and quantitative interaction energies useful to model the evolution of phosphorus and its effect in α Fe.

ACKNOWLEDGMENTS

The authors acknowledge fruitful discussions with Professor D.J. Bacon and Dr. A.V. Barashev. This work was initiated in the framework of the EDF REVE (virtual reactor) project which aimed at simulating the irradiation effects in structural materials. It is now under way within the European Union supported project PERFECT (FI6O-CT-2003-508840) and the ITEM network (FIR1-CT-2001-20163). Part of the calculations was done on the SP3 of the C.R.I. of the U.S.T.L. supported by the Fonds Européens de Développement Régional. Another part was done on the supercomputers at CCRT in the framework of an EDF-CEA contract.

[1] C. A. English, S. R. Ortner, G. Gage, W. L. Server, and S. T. Rosinski, *20th International Symposium*, ASTM STP 1405, edited by S. T. Rosinki, M. L. Grossbeck, T. R. Allen, and A. S. Kumar (ASTM West Conshohocken, PA, 2001).

[2] S. G. Druce, G. Gage, and G. Jordan, Acta Metall. **34**, 641 (1986).

[3] M. K. Miller and P. Pareige, Mater. Res. Soc. Symp. Proc. **650**, R6.1 (2001).

[4] Y. Nishiyama, T. E. Bloomer, and J. Kameda, Mater. Res. Soc. Symp. Proc. **650**, R6.10 (2001).

[5] M. K. Miller, P. Pareige, and M. G. Burke, Mater. Charact. **44**, 235 (2000).

[6] A. B. Lidiard, Philos. Mag. A **79**, 1493 (1999).

[7] A. Barbu and A. B. Lidiard, Philos. Mag. A **74**, 709 (1996).

[8] R. G. Faulkner, D. J. Bacon, S. Song, and P. E. J. Flewitt, J. Nucl. Mater. **271–272**, 1 (1999).

[9] A. D. Le Claire and G. Neumann, in *Numerical Data and Functional Relationship in Science and Technology*, edited by H. Me-

hrer, Landolt-Börnstein, New Series, Group III, Vol. 26, (Springer-Verlag, Berlin, 1990), Chap. 3, pp. 130–179.
[10] A. Hardouin du Parc, Ph.D. thesis, Paris XI-Orsay University, 1998.
[11] Y. Nagai, K. Takadate, Z. Tang, H. Ohkubo, H. Sunaga, H. Takizawa, and M. Hasegawa, Phys. Rev. B **67**, 224202 (2003).
[12] M. Hashimoto, Y. Ishida, R. Yamamoto, and M. Doyama, Acta Metall. **32**, 1 (1984).
[13] A. A. Vasiliev, V. V. Rybin, and A. A. Zisman, J. Nucl. Mater. **231**, 249 (1996).
[14] G. J. Ackland, D. J. Bacon, A. F. Calder, and T. Harry, Philos. Mag. A **75**, 713 (1997).
[15] S. M. J. Gordon, H. Hurchand, S. D. Kenny, and R. Smith, Nucl. Instrum. Methods Phys. Res. B **228**, 131 (2005).
[16] H. Hurchand, S. D. Kenny, and R. Smith, Nucl. Instrum. Methods Phys. Res. B **228**, 146 (2005).
[17] M. I. Mendelev, S. W. Han, D. J. Srolovitz, G. J. Ackland, D. Y. Sun, and M. Asta, Philos. Mag. **83**, 3977 (2003).
[18] G. J. Ackland, M. I. Mendelev, D. J. Srolovitz, S. Han, and A. V. Barashev, J. Phys.: Condens. Matter **16**, 1 (2004).
[19] C. Domain and C. S. Becquart, Phys. Rev. B **65**, 024103 (2002).
[20] C. Domain, C. S. Becquart, and J. Foct, Phys. Rev. B **69**, 144112 (2004).
[21] M. Hashimoto, Y. Ishida, S. Wakayama, R. Yamamoto, M. Doyama, and T. Fujiwara, Acta Metall. **32**, 13 (1984).
[22] S. Tang, A. J. Freeman, and G. B. Olson, Phys. Rev. B **47**, 2441 (1993).
[23] L. Zhong, R. Wu, A. J. Freeman, and G. B. Olson, Phys. Rev. B **55**, 11133 (1997).
[24] L. P. Sagert, G. B. Olson, and D. E. Ellis, Philos. Mag. B **77**, 871 (1998).
[25] P. Rez and J. R. Alvarez, Acta Mater. **47**, 4069 (1999).
[26] H. W. King, J. Mater. Sci. **1**, 79 (1966).
[27] G. Kresse and J. Hafner, Phys. Rev. B **47**, R558 (1993); **49**, 14251 (1994).
[28] G. Kresse and J. Furthmüller, Phys. Rev. B **54**, 11169 (1996).
[29] G. Kresse and J. Furthmüller, Comput. Mater. Sci. **6**, 15 (1996).
[30] D. Vanderbilt, Phys. Rev. B **41**, R7892 (1990); G. Kresse and J. Hafner, J. Phys.: Condens. Matter **6**, 8245 (1996).
[31] J. P. Perdew and Y. Wang, Phys. Rev. B **45**, 13244 (1991).
[32] G. Kresse and D. Joubert, Phys. Rev. B **59**, 1758 (1999); P. E. Blöchl, *ibid.* **50**, 17953 (1994).
[33] S. H. Vosko, L. Wilk, and M. Nusair, Can. J. Phys. **58**, 1200 (1980).
[34] H. J. Monkhorst and J. D. Pack, Phys. Rev. B **13**, 5188 (1976). In the original Monkhorst and Pack scheme, the k point mesh is always symmetric around the Γ point, whereas very often in our calculations we adopted grids centered at the Γ point.
[35] D. E. Jiang and E. A. Carter, Phys. Rev. B **67**, 214103 (2003).
[36] G. Kresse and D. Joubert, Phys. Rev. B **59**, 1758 (1999).
[37] C. Kittel, *Introduction to Solid State Physics*, 6th ed. (Wiley, New York, 1987).
[38] L. Pauling, *General Chemistry* (Dover, New York, 1988).
[39] H. Mehrer, N. Stolica and N. A. Stolwijk, in *Numerical Data and Functional Relationships in Science and Technology*, edited by H. Mehrer, Landolt-Börnstein, New Series, Group III, Vol. 26, (Springer-Verlag, Berlin, 1990), Chap. 2, pp. 73.
[40] H. Abe and E. Kuramoto, J. Nucl. Mater. **271–272**, 209 (1999).
[41] H. Watanabe, A. Aoki, H. Murakami, T. Muroga, and N. Yoshida, J. Nucl. Mater. **555–557**, 815 (1988).
[42] A. D. Le Claire, J. Nucl. Mater. **69&70,** 70 (1978).
[43] A. D. Le Claire, in *Physical Chemistry: An Advanced Treatise*, edited by H. Eyring (Academic Press, New York, 1970), Vol. 10, chap. 5.
[44] Y. Le Bouar and F. Soisson, Phys. Rev. B **65**, 094103 (2002).
[45] C. S. Becquart and C. Domain, Nucl. Instrum. Methods Phys. Res. B **202**, 44 (2002).
[46] J. Philibert, *Atom Movements, Diffusion and Mass Transport in Solids*, Les Editions de Physique (Les Ulis, 1991).
[47] G. H. Vineyard, J. Phys. Chem. Solids **3**, 121 (1957).
[48] W. M. Young and E. W. Elcock, Proc. Phys. Soc. **89**, 735 (1966).
[49] R. A. Johnson, Phys. Rev. **134**, A1329 (1964).
[50] C. C. Fu, F. Willaime, and P. Ordejón, Phys. Rev. Lett. **92**, 175503 (2004).